Jurnal Penginderaan Jauh dan Pengolahan Data Citra Digital Vol. 20 No. 2
ISSN: 1412-8098 (print), 2549-726X (online)

Evaluation of Dynamic Vertical Column Height Approach for Converting Sentinel-5P Data into Surface Pollutant Concentrations in Surabaya City

Mohammad Rifqi Alfarizi[a,*], Lalu Muhamad Jaelani[a],
[a]Department of Geomatics Engineering, Institut Teknologi Sepuluh Nopember (ITS), Surabaya 60111, Indonesia

***Corresponding author: 5016221031@student.its.ac.id**

Abstract. Urban air quality monitoring requires methods that are both comprehensive and cost-effective. Sentinel-5P TROPOMI satellite data are freely available; however, their units (mol/m²) cannot directly represent surface pollutant concentrations (µg/m³) without the Vertical Column Height (VCH) parameter, which is commonly assumed to be constant. This assumption contradicts the dynamic nature of the atmosphere. This study demonstrates that VCH is inherently dynamic through the integration of Sentinel-5P data with in-situ air quality sensor observations in Surabaya City. Daily VCH values were calculated for SO_2, CO, and NO_2 at the Kebonsari and Wonorejo monitoring stations throughout 2024 by pairing Vertical Column Density (VCD) data (retrieved via Google Earth Engine) with surface pollutant concentrations (obtained from the Surabaya Environmental Agency) based on matching dates and coordinates. The results show that VCH varies significantly on both daily and monthly scales, indicating that a static VCH assumption is not representative. The correlation between VCH and in-situ concentrations is negative, with the following order of strength: CO ($r = -0.7989$; $R^2 = 0.6383$) > NO_2 ($r = -0.5913$; $R^2 = 0.3496$) > SO_2 ($r = -0.3818$; $R^2 = 0.1457$), consistent with the atmospheric lifetime of each pollutant. Additional analysis shows that MODIS surface temperature shows weak positive correlations with VCH for all pollutants: SO_2 ($r = 0.2903$; $R^2 = 0.0843$) > CO ($r = 0.2464$; $R^2 = 0.0607$) > NO_2 ($r = 0.0033$; $R^2 \approx 0.0000$), indicating that surface temperature alone is insufficient to explain vertical pollutant distribution. A dynamic VCH approach is therefore necessary for more accurate satellite-to-surface pollutant conversion, and future models require integration of more comprehensive meteorological parameters.

Keywords: *Air Quality Sensor, Sentinel-5, Surabaya, Temporal Integration, Vertical Column Height.*

I. INTRODUCTION

Air quality monitoring in urban areas such as Surabaya is a critical environmental health issue. Population growth, industrialization, and increasing motor vehicle use have contributed to elevated concentrations of pollutants such as NO_2, CO, and SO_2 [1][2]. Conventional monitoring using in-situ sensors is limited by high installation costs and weak spatial coverage [3]. Sentinel-5P TROPOMI offers an alternative solution through its capability to provide free, daily, and global measurements of atmospheric pollutants [4]. However, Sentinel-5P data only provide Vertical Column Density (mol/m²), which cannot directly represent surface pollutant concentrations (µg/m³). A unit conversion method is therefore required. The Vertical Column Height (VCH) parameter is essential in this conversion, representing the effective height of the atmospheric column in which pollutants resided [5].

The main issue is that VCH is commonly assumed to be constant in many studies, for example 12 km for CO and 3 km for NO_2 [6]. This assumption contradicts the dynamic nature of the atmosphere, which is influenced by climate, seasonality, and local meteorological conditions [7]. In tropical regions such as Indonesia, VCH may fluctuate substantially due to diurnal cycles, atmospheric chemistry, and meteorological processes [8]. Therefore, the use of static VCH values may introduce large uncertainties in surface concentration estimates.

Integrating satellite observations with in-situ sensor measurements provides a more representative approach for estimating VCH. Satellite data offer broad spatial coverage, while in-situ data provide high-accuracy local validation, making them complementary [5]. By temporally integrating these two data sources, VCH can be empirically calculated for each synchronized data pair, producing a more realistic representation of VCH dynamics than constant assumptions [4][9].

This study aims to, calculate daily VCH values through temporal integration of Sentinel-5P and in-situ sensor data for SO_2, CO, and NO_2 at two monitoring stations in Surabaya during 2024, analyze the temporal distribution characteristics of VCH on daily and monthly scales, evaluate the statistical relationship between VCH and surface pollutant concentrations; and identify the tendency of the relationship between VCH and MODIS surface temperature as a supporting meteorological factor. The results are expected to demonstrate that VCH is dynamic and to provide a reference for more accurate satellite-to-surface conversion methods.

II. METHODOLOGY

2.1 Study Location

This study was conducted at two air quality monitoring stations operated by the Ministry of Environment and Forestry (KLHK) in Surabaya City. The study area is illustrated in **Fig.1**.

Figure 1. Study Location

Fig. 1 shows the locations of the two monitoring stations: the Kebonsari Village Office Station (7°19'41.42" S; 112°42'49.06" E) and the Wonorejo Nursery Garden Station (7°18'42.92" S; 112°47'21.29" E). These stations were selected based on the availability of complete observation records over a full one-year period.

2.2 Materials and Equipment

The software and hardware used in this study included a laptop for data processing, result analysis, and report preparation; Google Earth Engine (GEE) for acquiring and processing Sentinel-5P satellite data; geographic information system (GIS) software for spatial visualization and map layout preparation; and Microsoft Office 365 for quantitative data analysis, validation testing, and manuscript preparation.

The datasets used in this study consisted of three main components. First, daily surface pollutant concentration data (µg/m³) for SO_2, CO, and NO_2 were obtained from in-situ air quality sensors at both monitoring stations, provided by KLHK Surabaya. Second, Vertical Column Density (VCD) data (mol/m²) for SO_2, CO, and NO_2 were acquired from Sentinel-5P TROPOMI imagery through Google Earth Engine based on the coordinates of each monitoring station. Third, surface temperature data (°C) from MODIS Aqua were collected for both stations over the same observation period and used as a supporting meteorological variable in the additional analysis.

2.3 Data Processing Methodology

The data processing workflow in this study consisted of several stages, as illustrated in **Fig. 2**. Google Earth Engine was used as the primary platform for data acquisition. Sentinel-5P satellite data for SO_2, CO, and NO_2 columns were retrieved and filtered for the January–December 2024 period to match the study timeframe.

The processing began with data cleaning and quality filtering applied independently to both datasets. For in-situ sensor data, records with negative values (indicating sensor malfunction), null entries (representing unrecorded observations), and near-zero values below the instrument detection limit were removed.

For satellite-derived VCD data, only pixels with valid quality assurance flags were retained. It should be noted that the spatial resolution of Sentinel-5P TROPOMI (3.5 × 5.5 km per pixel for SO_2 and NO_2; 7 × 7 km for CO) differs substantially from the point-based in-situ measurements, meaning each satellite pixel integrates atmospheric information over a much larger area than the sensor footprint.

Similarly, the temporal resolution differs. Satellite observations represent a single overpass snapshot (approximately 13:30 local time for the ascending node), whereas in-situ sensors record continuous daily averages. These resolution differences may introduce spatial representativeness errors, particularly for short-lived pollutants whose concentrations vary significantly within a single satellite pixel. This was followed by temporal integration, in which in-situ sensor observations and satellite-derived VCD values were paired based on exact date matching (same calendar day) and the geographic coordinates of each monitoring station. No temporal window or spatial buffer was applied; only data pairs sharing the same observation date and station coordinates were retained for analysis.

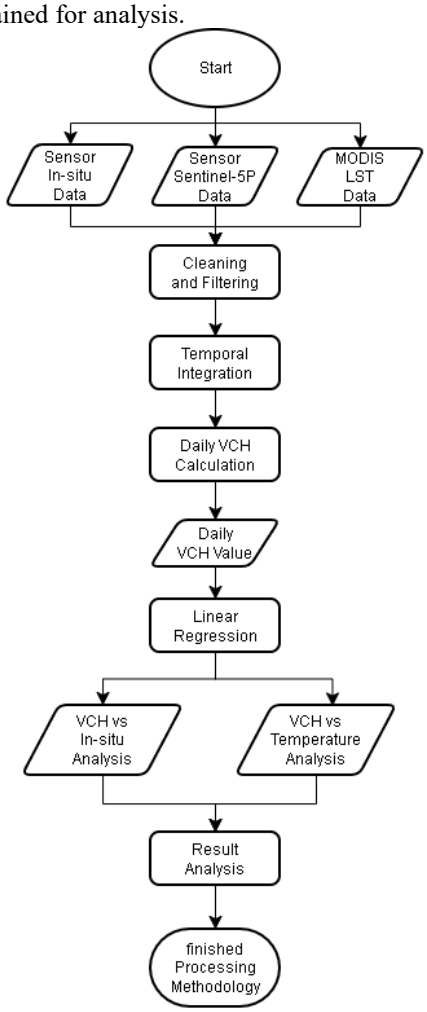

Figure 2. Processing Flow Diagram

Where VCD represents the amount of pollutant in the atmospheric column (mol/m²), and M is the molar mass of each pollutant: SO_2 = 64.07 g/mol, CO = 28.01 g/mol, and NO_2 = 46.01 g/mol. This empirical approach enables VCH estimation without requiring external meteorological data or a Chemical Transport Model [10]. Assuming that pollutants are homogeneously distributed within a vertical atmospheric column of height VCH, the surface concentration C(µg/m³) can be expressed as **Eq. 1** [11][12]:

$$SC_i = \frac{VCD \times M \times 10^6}{VCH\ (m)}\ [\mu g\ m^{-3}] \quad (1)$$

where SC_i is the surface pollutant concentration (µg/m³) measured by the in-situ sensor. Rearranging Equation (2), VCH can be defined as:

$$VCH = \frac{VCD \times M \times 10^6(\mu g\ m^{-2})}{SC_i(\mu g\ m^{-3})} \quad (2)$$

The VCH (m) obtained through this empirical approach represents the effective pollutant column height under the assumption of homogeneous pollutant distribution under idealized conditions. Daily VCH values were aggregated into monthly statistics, including mean, minimum, maximum, median, and number of valid observations.

Trend analysis was performed using Pearson correlation (r) and simple linear regression between two variables. The Pearson correlation coefficient was calculated as follows:

$$r = \frac{n \sum xy - (\sum x)(\sum y)}{\sqrt{[n \sum x^2 - (\sum x)^2][n \sum y^2 - (\sum y)^2]}} \quad (4)$$

Statistical analysis was conducted using simple linear regression ($Y = a + bX$) and Pearson correlation [21][22] for two relationships: (1) VCH versus in-situ concentration, to evaluate the relationship between vertical pollutant distribution and surface concentration, with data from both stations combined for each pollutant; and (2) VCH versus MODIS Aqua surface temperature, to identify the influence of meteorological factors. The strength of the relationships was evaluated using the correlation coefficient (r) and coefficient of determination (R^2) [13][14].

From the second regression analysis, an exploratory empirical model was formulated to describe the relationship between VCH and temperature for each pollutant using the general form:

$$VCH_{Polutan} = a + b \times T \quad (5)$$

where $T$is MODIS Aqua surface temperature (°C), $a$is the intercept (m), and $b$is the regression coefficient representing the change in VCH (m) per 1°C increase in temperature. This model was not intended as a primary predictive model, but rather as an exploratory approach to understand the tendency of temperature influence on the vertical distribution of atmospheric pollutants, consistent with the study limitation that comprehensive meteorological parameters were not included in the model.

III. RESULTS AND DISCUSSION

3.1 Temporal Characteristics of Each VCH Values

Daily VCH values were calculated throughout the 12-month observation period (2024) using Equation (3) for each valid data pair across the three pollutants at both monitoring stations. To facilitate interpretation, daily values were aggregated into monthly statistics including the number of valid observations (n), mean, minimum, maximum, and median. The monthly VCH statistical summaries for each pollutant are presented in **Tab. 1–3**.

Table 1. Monthly Statistical Summary of SO_2 (meter)

Months	Kebonsari			Wonorejo		
	n	x̄	Med	n	x̄	Med
January	2	1,718	1,718	2	823	823
February	3	1,811	2,254	7	2,442	2,101
March	2	2,085	2,085	6	1,711	1,337
April	6	3,888	2,562	4	2,215	1,813
May	19	1,681	1,549	21	2,427	1,451
June	14	2,430	2,377	15	1,650	941
July	21	4,782	4,753	22	2,459	2,459
August	20	1,943	1,780	0	—	—
September	13	2,224	2,516	0	—	—
October	15	5,313	5,313	0	—	—
November	8	2,635	1,984	0	—	—
December	1	1,273	1,273	2	2,601	1,372

Table Description: n = amount of monthly data avaibility; x̄ = Mean; Med = median

Based on **Tab. 1**, SO_2 VCH exhibits the most significant fluctuations among the three pollutants. At Kebonsari Station, valid observations were relatively complete, especially from May to October, with the highest average VCH observed in October (5,313 m) and the lowest in December (1,273 m). At Wonorejo Station, valid observations were more limited and absent from August to November. These data gaps were caused by null values in the in-situ sensor records, preventing temporal pairing with satellite observations. The limited number of valid observations, particularly the complete absence of data from August to November at Wonorejo, means that the SO_2 results should be interpreted with caution, as they may not fully represent the annual variability of SO_2 VCH at this station.

The high variability of SO_2 VCH is explained by the atmospheric behavior of SO_2, which has a very short atmospheric lifetime, typically ranging from hours to a few days, making its distribution highly dependent on local emission sources and atmospheric conditions at the time of observation [15][16]. The relatively low sensitivity of satellite SO_2 detection at low concentrations also

contributed to the limited number of valid observations, as many records failed quality filtering [17].

Table 2. Monthly Statistical Summary of CO VCH (m)

Month	Kebonsari			Wonorejo		
	n	x̄	Med	n	x̄	Med
January	11	322,459	320,686	9	150,900	140,542
February	15	327,852	337,068	14	160,634	157,527
March	5	632,932	437,395	4	812,272	819,879
April	6	921,725	849,910	9	823,692	794,329
May	23	969,912	879,023	22	850,412	860,413
June	25	560,199	515,602	15	773,165	791,015
July	21	470,734	447,307	20	728,705	711,842
August	10	637,179	634,912	21	830,967	776,196
September	6	571,382	476,137	13	849,863	797,231
October	10	874,416	827,122	18	1,085,000	1,071,716
November	8	704,201	684,294	11	969,921	956,121
December	5	197,769	211,732	10	727,051	717,410

Description: n = amount of monthly data avaibility; x̄ = Mean; Med = median

Based on **Tab.2** CO VCH exhibited a markedly different pattern. The magnitude of CO VCH was substantially higher than that of SO_2 and NO_2, reaching hundreds of thousands of meters, with a more stable monthly distribution. At Wonorejo Station, a clear increasing trend was observed from March (812,272 m) to a peak in October (1,084,999 m), suggesting pollutant accumulation during the dry season.

The large CO VCH values are consistent with the atmospheric characteristics of CO, which has a relatively long atmospheric lifetime, ranging from weeks to months, and low chemical reactivity [17]. These properties allow CO to become more uniformly distributed both vertically and horizontally throughout the atmospheric column. The fundamental difference between satellite observations, which capture the total pollutant load across the full atmospheric column, and in-situ measurements, which only represent surface concentrations, explains why CO yields much larger VCH values. This reinforces the importance of using an appropriate VCH parameter when converting satellite column data to surface concentrations.

Table 3. Monthly Statistical Summary VCH NO_2 (meter)

Months	Kebonsari			Wonorejo		
	n	x̄	Med	n	x̄	Med
January	26	504	427	26	178	151
February	25	345	342	24	200	159
March	25	454	370	27	756	463
April	24	1.095	630	23	314	254
May	28	421	335	31	209	200
June	26	1.214	963	28	257	259
July	24	1.507	1.211	30	238	218
August	27	846	654	30	273	214
September	27	715	447	30	231	227
October	31	917	373	31	230	220
November	29	483	336	27	222	210
December	20	392	394	23	435	399

Description: n = amount of monthly data avaibility; x̄ = Mean; Med = median

NO_2 VCH had the most consistent number of valid observation pairs among the three pollutants, with a relatively even distribution throughout the year. At Kebonsari Station, fluctuations were pronounced, with a substantial increase in June (1,214 m) and July (1,507 m). In contrast, Wonorejo Station showed a more stable pattern, with monthly mean values ranging from 178 m (January) to 756 m (March).

This relative stability is attributed to the continuous nature of NO_2 emissions, primarily from motor vehicle traffic and industrial activities that occur almost continuously . However, NO_2 remains chemically reactive, meaning its distribution is influenced not only by emission intensity but also by photochemical reactions and atmospheric transport processes.

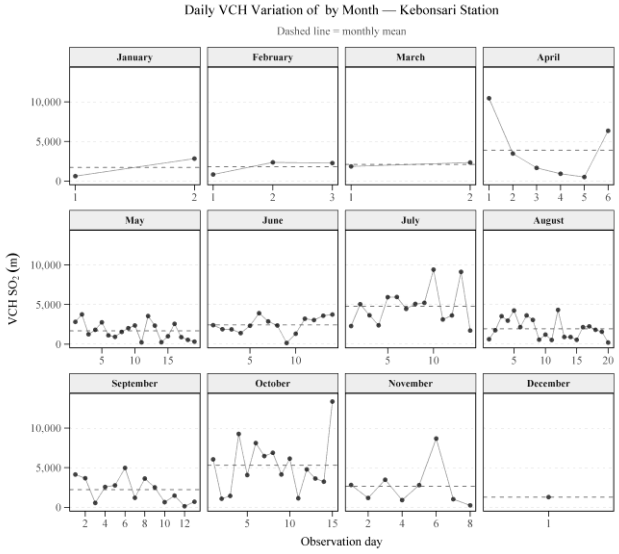

Figure 3. Daily Variation of VCH SO_2 — Kebonsari

Fig. 3 shows the daily variation of SO_2 VCH at Kebonsari Station. Sharp spikes appear sporadically in almost every month. In April, one observation exceeded 10,000 m, and a similar pattern occurred again in October. December contained only a single valid observation. The monthly mean line also shows clear inter-month variation, ranging from approximately 1,700 m in May to 5,300 m in October).

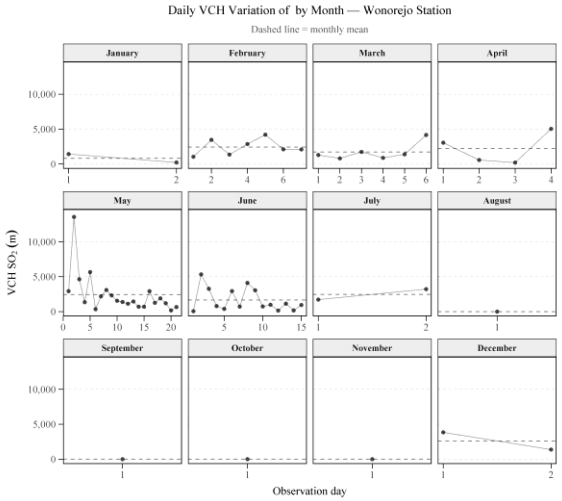

Figure 4. Daily Variation of VCH SO_2 — Wonorejo

Fig. 4 presents the daily variation of SO_2 VCH at Wonorejo Station, showing an even more contrasting pattern. In May, one extreme spike exceeded 13,000 m, while most other observations remained within the 500–3,000 m range. The September–November panels are empty due to the absence of valid observations. This extreme variability is consistent with the short atmospheric lifetime of SO_2. reported that SO_2 lifetime typically ranges from several hours to one day, making it highly sensitive to local emissions. [6]further noted that TROPOMI SO_2 retrieval performance strongly depends on emission intensity, which explains why many low-concentration observations fail quality filtering [17].

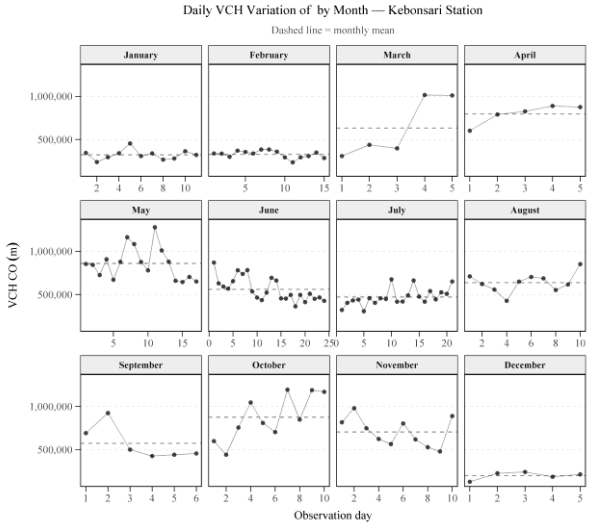

Figure 5. Daily Variation of VCH CO — Kebonsari

Fig. 5 illustrates daily CO VCH variation at Kebonsari Station. Compared with SO_2, CO exhibits much more moderate fluctuations. The May panel contains the highest number of valid observations (23 points), with values ranging from 644,000 to 1,574,000 m. No single extreme outlier is observed; instead, the fluctuations are more continuous and regular throughout the month.

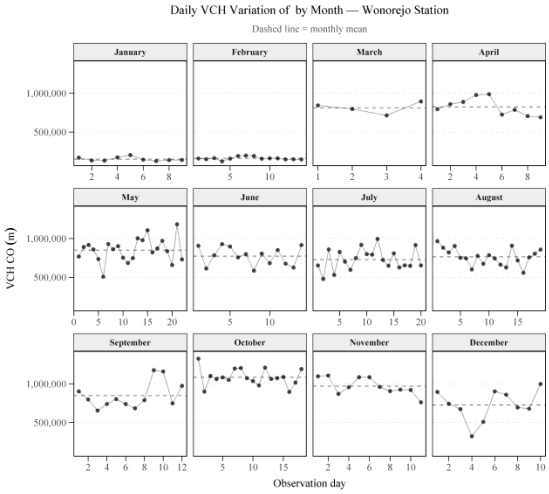

Figure 6. Daily Variation of VCH CO — Wonorejo

Fig. 6 shows daily CO VCH variation at Wonorejo Station and confirms a seasonal pattern. January–February values are concentrated within 120,000–200,000 m, followed by a progressive increase toward October (894,000–1,324,000 m), while maintaining relatively stable daily variability. This stability is consistent with the long atmospheric lifetime and low reactivity of CO. Edwards et al. (2006) explained that CO has strong long-range transport capability and broad atmospheric distribution due to its long atmospheric residence time [17]. The high CO VCH values are also explained by the difference between satellite observations, which capture the full atmospheric column, and in-situ sensors, which only represent near-surface conditions.

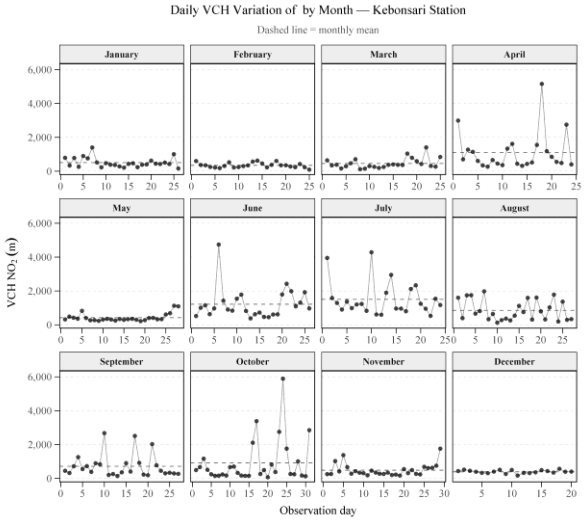

Figure 7. Daily Variation of VCH NO_2 — Kebonsari

Fig. 7 shows the daily variation of NO_2 VCH at

Kebonsari Station. Compared with SO_2 and CO, NO_2 displays more dynamic but less extreme fluctuations. In April, one observation exceeded 5,000 m, while in June–July several observations exceeded 3,000–4,000 m. In October, which contains the highest number of observations (31 points), one outlier approached 6,000 m, clearly contrasting with the majority of values below 1,000 m.

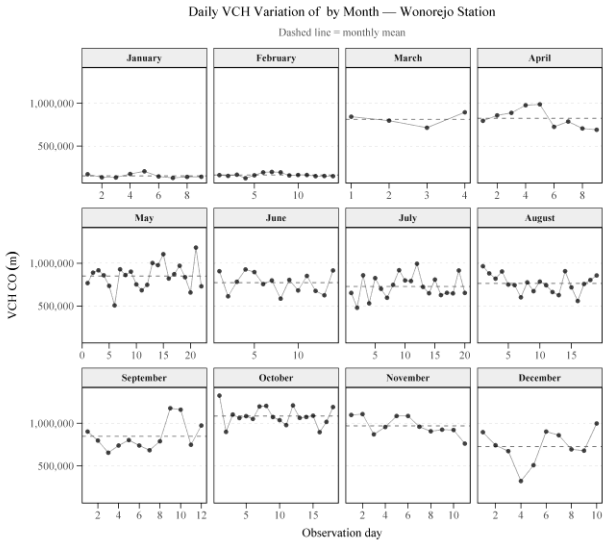

Figure 8. Daily Variation of VCH NO_2 — Wonorejo

Fig. 8 shows the daily variation of NO_2 VCH at Wonorejo Station. In contrast to Kebonsari, NO_2 at Wonorejo is highly stable, with nearly all observations from May to November remaining within a narrow range of 120–450 m and a nearly flat monthly mean line. This stability is explained by the continuous nature of NO_2 emissions from transportation and industrial activities. NO_2 distribution is governed by both emissions and photochemical reactions, resulting in a more continuous spatial and temporal pattern than SO_2 [18].

The difference between stations indicates that Kebonsari, characterized by denser traffic and industrial activity, experiences more variable pollutant accumulation than Wonorejo. Overall, the distribution and daily variation of VCH reveal three major findings: (1) VCH values vary significantly on both daily and monthly scales, confirming that a static VCH assumption is not representative; (2) VCH values at two stations within the same city differ substantially at the same time, highlighting the strong influence of local atmospheric conditions; and (3) the degree of variability follows the order SO_2 > CO > NO_2, corresponding to pollutant reactivity and atmospheric lifetime. These findings are emphasized that atmospheric column height is dynamic and varies with atmospheric conditions [19].

3.2 Relationship Analysis Between VCH and Surface Pollutant Concentration

The relationship between VCH and surface pollutant concentration was analyzed using simple linear regression and Pearson correlation by combining data from both stations for each pollutant. Conceptually, VCH is inversely related to surface concentration: as VCH increases, surface concentration decreases due to stronger vertical dilution. However, this relationship is also influenced by emission variability, pollutant transport, and atmospheric dynamics.

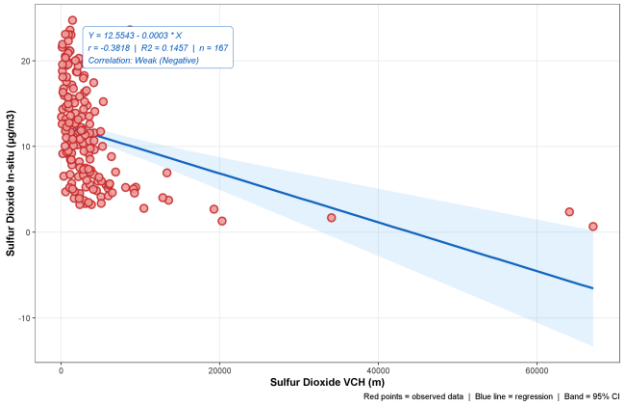

Figure 9. Regression Scatter Plot VCH vs In-situ Concentration SO_2

Fig. 9 shows the regression between SO_2 VCH and in-situ SO_2 concentration. The resulting regression equation is Y = 12,5543 − 0,0003X with a Pearson correlation coefficient of $r = -0.3818$ and $R^2 = 0.1457$, based on 167 valid observation pairs. This weak negative correlation reflects the highly unstable atmospheric behavior of SO_2. Its short atmospheric lifetime and strong dependence on local emissions reduce the consistency between column distribution and surface concentration [20]. SO_2 is also rapidly oxidized into sulfate aerosols , further weakening the direct relationship between VCH and surface-level SO_2 concentration.

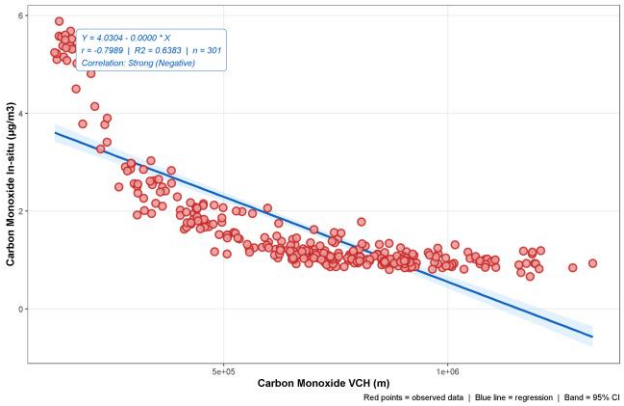

Figure 10. Regression Scatter Plot VCH vs In-situ Concentration CO

Fig. 10 presents the regression between CO VCH and in-situ CO concentration. The resulting regression equation is Y = 4,0304 − 0,0000X with $r = -0.7989$ and $R^2 = 0.6383$, based on 301 valid observation pairs. This strong negative correlation reflects the relatively stable atmospheric behavior of CO, which has a long atmospheric lifetime and low chemical reactivity [21]. Approximately 63.83% of the variation in surface CO concentration can be explained by VCH, indicating that, within the context of

this study area and dataset, CO is the most suitable pollutant for VCH-based surface estimation. However, this finding should be interpreted with caution, as the strength of this relationship may vary in other geographical and climatic settings.

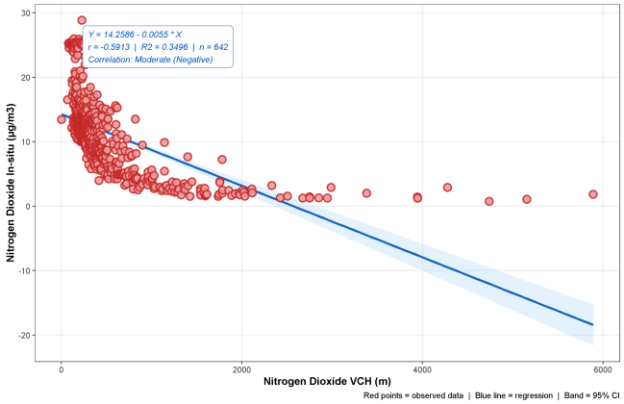

Figure 11. Regression Scatter Plot VCH vs In-situ Concentration NO_2

Fig. 11 shows the regression between NO_2 VCH and in-situ NO_2 concentration. The resulting regression equation is Y = 14,2586 − 0,0055X with $r = -0.5913$ and $R^2 = 0.3496$, based on 642 valid observation pairs. This moderate negative correlation suggests that NO_2 has a measurable but less stable relationship between vertical column distribution and surface concentration. NO_2 has an atmospheric lifetime ranging from several hours to approximately one day and actively participates in the NOx photochemical cycle, including photolysis and tropospheric ozone formation [21]. [22] reported that the relationship between satellite column and surface NO_2 is highly sensitive to atmospheric conditions. The moderate R^2value indicates that surface NO_2 variability remains strongly controlled by local emissions [23].

The resulting correlation ranking is, CO ($r = -0.7989$) > NO_2 ($r = -0.5913$) > SO_2 ($r = -0.3818$). This order directly corresponds to the atmospheric lifetime and chemical reactivity of each pollutant. Pollutants with longer atmospheric lifetimes and lower chemical reactivity are more evenly distributed throughout the atmospheric column, resulting in a stronger and more consistent relationship between VCH and surface concentration. This difference is also influenced by the dominant emission scale: CO reflects regional accumulation, NO_2 represents an intermediate scale, and SO_2 is dominated by highly localized emissions. It is important to note that these correlations describe statistical associations and do not necessarily imply direct causal mechanisms. The observed negative relationships are consistent with the theoretical framework of vertical dilution, but multiple confounding factors, including emission variability, horizontal transport, and atmospheric chemistry, may simultaneously influence both VCH and surface concentrations. The results presented here are specific to the Surabaya urban context and the 2024 observation period; generalization to other regions or time periods should be made with appropriate caution.

3.3 Relationship Analysis Between VCH and MODIS Surface Temperature

The relationship between VCH and MODIS Aqua surface temperature was analyzed as an additional assessment to identify the tendency of meteorological influence on pollutant vertical distribution. Surface temperature plays a role in controlling vertical atmospheric mixing. Higher temperatures generally enhance convection and turbulence, allowing pollutants to disperse into higher atmospheric layers and potentially increasing VCH. Canché-Cab et al. (2024) reported that unstable atmospheric conditions induced by surface heating promote stronger vertical pollutant mixing [24]. Conversely, lower temperatures tend to suppress vertical mixing, causing pollutants to accumulate near the surface [25].

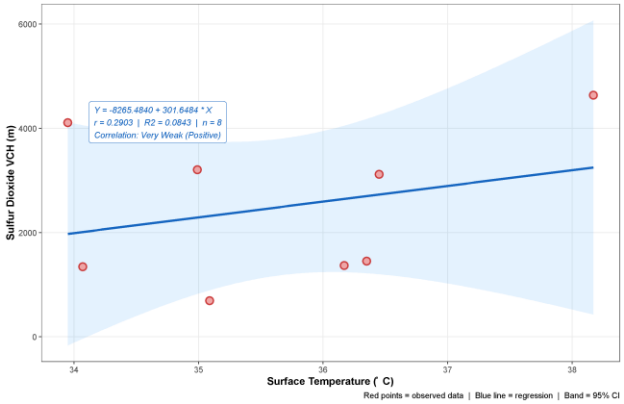

Figure 12. Regression Scatter Plot VCH SO_2 vs Surface Temperature

Fig. 12 shows the regression between SO_2 VCH and MODIS surface temperature. The resulting regression equation is: Y = −8.265,4840 + 301,6484X with $r = 0.2903$ and $R^2 = 0.0843$, based on 8 valid observation pairs. This weak positive correlation suggests that increasing temperature tends to coincide with higher SO_2 VCH, but the relationship remains limited. Only 8.43% of SO_2 VCH variability can be explained by temperature, while the remaining variation is controlled by other factors. [26] explained that the influence of temperature on SO_2 vertical distribution is limited because SO_2 remains strongly controlled by surface emission intensity. [27] also noted that only a small fraction of SO_2 is transported into higher atmospheric layers. The small sample size further limits the reliability of this relationship.

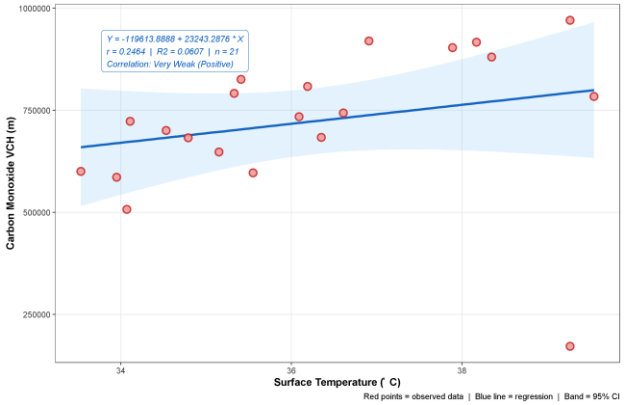

Figure 13. Regression Scatter Plot VCH CO vs Surface Temperature

Fig. 13 shows the regression between CO VCH and MODIS surface temperature. The resulting regression equation is Y = −119.613,8888 + 23.243,2876X with $r = 0.2464$ and $R^2 = 0.0607$, based on 21 valid observation pairs. This very weak positive correlation does not support the expectation that CO would respond strongly to temperature-driven vertical mixing. At the local scale of Surabaya, other factors appear to be more influential. [28] showed that CO variability is strongly affected by long-range horizontal transport, while [29] emphasized that CO distribution is controlled by a complex interaction of emissions, atmospheric transport, and chemical processes.

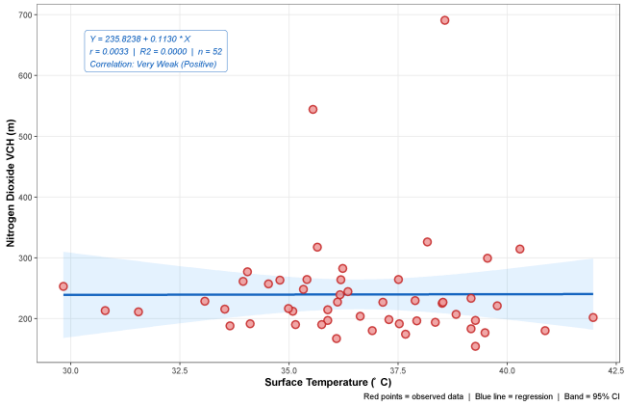

Figure 14. Regression Scatter Plot VCH NO_2 vs Surface Temperature

Fig. 14 shows the regression between NO_2 VCH and MODIS surface temperature. The resulting regression equation is Y = 235,8238 + 0,1130X with $r = 0.0033$ and $R^2 \approx 0.0000$, based on 52 valid observation pairs. This near-zero correlation indicates that no meaningful linear relationship exists between surface temperature and NO_2 vertical distribution in Surabaya. This result is consistent with the chemical behavior of NO_2 as a highly reactive and short-lived pollutant.

NO_2 distribution is dominated by local emissions from transportation and industrial activity, which fluctuate independently of temperature. NO_2 is also actively involved in photochemical cycling, causing rapid concentration changes that are not directly governed by temperature alone [30]. Further reported that NO_2 variability in urban regions is more strongly controlled by anthropogenic emissions than by meteorological parameters [31].

The correlation ranking between VCH and temperature is: SO_2 ($r = 0.2903$) > CO ($r = 0.2464$) > NO_2 ($r = 0.0033$). All three pollutants show weak to negligible correlations, indicating that surface temperature alone has very limited influence on pollutant vertical distribution in Surabaya. A temperature-only approach is therefore insufficient, and additional meteorological, physical, and chemical variables are required for more comprehensive analysis. Furthermore, it should be noted that the temperature data used in this study represents Land Surface Temperature (LST) from MODIS Aqua, which is physically distinct from air temperature. Good et al. (2017) demonstrated that LST and air temperature can differ by 5–10°C in urban areas during daytime due to the urban heat island effect [32]. Since vertical mixing processes in the atmosphere are more directly related to air temperature profiles than to surface material temperature, the use of LST as a proxy may have contributed to the weak correlations observed. The limited number of valid temperature-VCH pairs (n = 8 for SO_2, n = 21 for CO, n = 52 for NO_2) further constrains the statistical power of these analyses, and the resulting conclusions should therefore be interpreted as preliminary and exploratory rather than definitive.

A. Empirical VCH-Temperature Model Development

Based on the regression analysis, empirical VCH–temperature models were developed using Equation (5). These models are exploratory and intended to describe the tendency of temperature influence on pollutant vertical distribution rather than serve as primary predictive models.

The empirical model for carbon monoxide is:

$$VCH_{CO} = -119.613,8888 + 23.243,2876\ T \quad (6)$$
$$(R^2 = 0,0607)$$

Although the regression coefficient suggests that CO VCH increases by 23,243 m for every 1°C increase in surface temperature, the very low R^2value indicates that this model explains only 6.07% of CO VCH variability. This confirms that CO vertical distribution is more strongly controlled by horizontal transport and emission variability than by temperature.

The empirical model for sulfur dioxide is:

$$VCH_{SO_2} = -8.265,4840 + 301,6484\ T \quad (7)$$
$$(R^2 = 0,0843)$$

The low R^2value indicates that the model explains only 8.43% of SO_2 VCH variability. This confirms that SO_2 vertical distribution is more strongly governed by local emissions and atmospheric chemical processes than by temperature. The limited number of valid observations also reduces model reliability.

The empirical model for nitrogen dioxide is:

$$VCH_{NO_2} = 235,8238 + 0,1130\ T \quad (8)$$
$$(R^2 = 0,0000)$$

The NO_2 model shows virtually no explanatory power. The regression coefficient is only 0.1130 m per 1°C, which

is practically negligible. Although this model is supported by the largest number of valid observations, it has no meaningful predictive capability.

Overall, the three empirical models confirm that surface temperature alone is not sufficient to explain VCH variability in Surabaya. These results reinforce the need for multivariate approaches that integrate additional meteorological and atmospheric parameters, such as boundary layer height, wind speed, humidity, and photochemical intensity, to better characterize pollutant vertical distribution.

IV. CONCLUSION

The temporal integration method between Sentinel-5P and in-situ sensor data was successfully implemented through synchronization of observation dates and coordinates, producing valid daily VCH pairs for SO_2 (167 pairs), CO (301 pairs), and NO_2 (642 pairs). The calculated VCH values varied significantly on both daily and monthly scales for all three pollutants at both monitoring stations. The degree of variability followed the order SO_2 > CO > NO_2, corresponding to the chemical reactivity and atmospheric lifetime of each pollutant. VCH values at the two stations within the same city also differed substantially at the same time, demonstrating that the static VCH approach commonly used in previous studies is not representative of real atmospheric conditions.

The relationship between VCH and in-situ concentration showed a negative correlation with the order: CO ($r = -0.7989$; $R^2 = 0.6383$) > NO_2 ($r = -0.5913$; $R^2 = 0.3496$) > SO_2 ($r = -0.3818$; $R^2 = 0.1457$). This ranking directly reflects atmospheric lifetime and chemical reactivity. Long-lived, less reactive pollutants exhibit more homogeneous vertical distributions, resulting in stronger and more consistent relationships between VCH and surface concentration. VCH can therefore serve as a robust surface concentration indicator for CO, a moderately representative indicator for NO_2, and a weak indicator for SO_2 unless additional variables such as local emissions and meteorological conditions are incorporated.

The additional analysis of MODIS surface temperature showed weak positive correlations for all pollutants: SO_2 ($r = 0.2903$; $R^2 = 0.0843$) > CO ($r = 0.2464$; $R^2 = 0.0607$) > NO_2 ($r = 0.0033$; $R^2 \approx 0.0000$). The empirical VCH–temperature models developed in this study showed no meaningful predictive capability for any pollutant. These findings indicate that surface temperature alone is insufficient to explain vertical pollutant distribution in Surabaya. Overall, this study confirms that a dynamic VCH approach is necessary for more accurate satellite column-to-surface conversion and that future predictive models require multivariate integration of more comprehensive meteorological and atmospheric parameters.

ACKNOWLEDGEMENT

The authors would like to thank KLHK Surabaya for providing air quality monitoring data.

REFERENCES

[1] B. Mamtimin and F. X. Meixner, “Air pollution and meteorological processes in the growing dryland city of Urumqi (Xinjiang, China),” *Science of The Total Environment*, vol. 409, no. 7, pp. 1277–1290, 2011, doi: https://doi.org/10.1016/j.scitotenv.2010.12.010.

[2] A. D. Syafei, A. Fujiwara, and J. Zhang, “Spatial and Temporal Factors of Air Quality in Surabaya City: An Analysis based on a Multilevel Model,” *Procedia Soc. Behav. Sci.*, vol. 138, pp. 612–622, Jul. 2014, doi: 10.1016/j.sbspro.2014.07.246.

[3] M. Santoso *et al.*, “Assessment of Urban Air Quality in Indonesia,” *Aerosol Air Qual. Res.*, vol. 20, pp. 2142–2158, 2020, doi: 10.4209/aaqr.2019.09.0451.

[4] C. Morillas, S. Alvarez, J. C. M. Pires, A. J. Garcia, and S. Martinez, “Impact of the implementation of Madrid’s low emission zone on NO2 concentration using Sentinel-5P/TROPOMI data,” *Atmos. Environ.*, vol. 320, p. 120326, 2024, doi: https://doi.org/10.1016/j.atmosenv.2024.120326.

[5] A. Cofano, F. Cigna, L. S. Amato, M. S. de Cumis, and D. Tapete, “Exploiting sentinel-5p tropomi and ground sensor data for the detection of volcanic so2 plumes and activity in 2018–2021 at Stromboli, Italy,” *Sensors*, vol. 21, no. 21, Nov. 2021, doi: 10.3390/s21216991.

[6] N. Theys *et al.*, “Sulfur dioxide vertical column DOAS retrievals from the Ozone Monitoring Instrument: Global observations and comparison to ground-based and satellite data,” *J. Geophys. Res.*, vol. 120, no. 6, pp. 2470–2491, 2015, doi: 10.1002/2014JD022657.

[7] M. A. Rahman *et al.*, “Weather radar detection of planetary boundary layer and smoke layer top of peatland fire in Central Kalimantan, Indonesia,” *Sci. Rep.*, vol. 11, no. 1, Dec. 2021, doi: 10.1038/s41598-020-79486-6.

[8] L. H. Yang *et al.*, “Tropospheric NO2vertical profiles over South Korea and their relation to oxidant chemistry: implications for geostationary satellite retrievals and the observation of NO2diurnal variation from space,” *Atmos. Chem. Phys.*, vol. 23, no. 4, pp. 2465–2481, Feb. 2023, doi: 10.5194/acp-23-2465-2023.

[9] T. Verhoelst *et al.*, “Ground-based validation of the Copernicus Sentinel-5P TROPOMI NO2 measurements with the NDACC ZSL-DOAS, MAX-DOAS and Pandonia global networks,” *Atmos.*

Meas. Tech., vol. 14, no. 1, pp. 481–510, Jan. 2021, doi: 10.5194/amt-14-481-2021.

[10] D. L. Goldberg, S. C. Anenberg, D. Griffin, C. A. McLinden, Z. Lu, and D. G. Streets, "Disentangling the Impact of the COVID-19 Lockdowns on Urban NO2 From Natural Variability," *Geophys. Res. Lett.*, vol. 47, no. 17, Sep. 2020, doi: 10.1029/2020GL089269.

[11] D. Jacob, *INTRODUCTION TO ATMOSPHERIC CHEMISTRY: SUPPLEMENTAL QUESTIONS AND PROBLEMS*, 11th ed. Princeton University Press, 1999.

[12] P. W. Atkins and J. De Paula, *Physical chemistry : thermodynamics, structure, and change*, 10th ed. 2014.

[13] H. Akoglu, "User's guide to correlation coefficients," Sep. 01, 2018, *Emergency Medicine Association of Turkey*. doi: 10.1016/j.tjem.2018.08.001.

[14] A. Schneider, G. Hommel, and M. Blettner, "Lineare regressionsanalyse - Teil 14 der serie zur bewertung wissenschaftlicher publikationen," Nov. 05, 2010. doi: 10.3238/arztebl.2010.0776.

[15] N. A. Krotkov *et al.*, "Aura OMI observations of regional SO2 and NO2 pollution changes from 2005 to 2015," *Atmos. Chem. Phys.*, vol. 16, no. 7, pp. 4605–4629, Apr. 2016, doi: 10.5194/acp-16-4605-2016.

[16] N. Theys *et al.*, "Sulfur dioxide retrievals from TROPOMI onboard Sentinel-5 Precursor: Algorithm theoretical basis," *Atmos. Meas. Tech.*, vol. 10, no. 1, pp. 119–153, Jan. 2017, doi: 10.5194/amt-10-119-2017.

[17] D. P. Edwards *et al.*, "Satellite-observed pollution from Southern Hemisphere biomass burning," *Journal of Geophysical Research Atmospheres*, vol. 111, no. 14, Jul. 2006, doi: 10.1029/2005JD006655.

[18] M. Kazemi Garajeh, G. Laneve, H. Rezaei, M. Sadeghnejad, N. Mohamadzadeh, and B. Salmani, "Monitoring Trends of CO, NO2, SO2, and O3 Pollutants Using Time-Series Sentinel-5 Images Based on Google Earth Engine," *Pollutants*, vol. 3, no. 2, pp. 255–279, Jun. 2023, doi: 10.3390/pollutants3020019.

[19] S. Shetty, P. Schneider, K. Stebel, P. David Hamer, A. Kylling, and T. Koren Berntsen, "Estimating surface NO2 concentrations over Europe using Sentinel-5P TROPOMI observations and Machine Learning," *Remote Sens. Environ.*, vol. 312, p. 114321, 2024, doi: https://doi.org/10.1016/j.rse.2024.114321.

[20] V. E. Fioletov, C. A. McLinden, N. Krotkov, and C. Li, "Lifetimes and emissions of SO2 from point sources estimated from OMI," *Geophys. Res. Lett.*, vol. 42, no. 6, pp. 1969–1976, Mar. 2015, doi: 10.1002/2015GL063148.

[21] T. Holloway, H. Levy, and P. Kasibhatla, "Global distribution of carbon monoxide," *Journal of Geophysical Research Atmospheres*, vol. 105, no. D10, pp. 12123–12147, May 2000, doi: 10.1029/1999JD901173.

[22] L. N. Lamsal *et al.*, "Evaluation of OMI operational standard NO2 column retrievals using in situ and surface-based NO2 observations," *Atmos. Chem. Phys.*, vol. 14, no. 21, pp. 11587–11609, Nov. 2014, doi: 10.5194/acp-14-11587-2014.

[23] D. L. Goldberg *et al.*, "NO $_2$ concentration differences under clear versus cloudy skies and implications for applications of satellite measurements," Apr. 15, 2025. doi: 10.5194/egusphere-2025-1350.

[24] L. Canché-Cab, L. San-Pedro, B. Ali, M. Rivero, and M. Escalante, "The atmospheric boundary layer: a review of current challenges and a new generation of machine learning techniques," *Artif. Intell. Rev.*, vol. 57, no. 12, Dec. 2024, doi: 10.1007/s10462-024-10962-5.

[25] N. S. Berman, H. J. S. Fernando, E. Pardyjak, F. Yu, A. Mahalov, and A. Grachev, "A study of the turbulent mixing in the atmospheric boundary layer of phoenix, Arizona," *Proceedings of the 1999 3rd ASME/JSME Joint Fluids Engineering Conference, FEDSM'99, San Francisco, California, USA, 18-23 July 1999 (CD-ROM)*, p. 1, 1999, [Online].

[26] A. P. Cuesta-Mosquera, M. Wahl, J. G. Acosta-López, J. A. García-Reynoso, and B. H. Aristizábal-Zuluaga, "Mixing layer height and slope wind oscillation: Factors that control ambient air SO2 in a tropical mountain city," *Sustain. Cities Soc.*, vol. 52, p. 101852, 2020, doi: https://doi.org/10.1016/j.scs.2019.101852.

[27] I. Faloona *et al.*, "Sulfur dioxide in the tropical marine boundary layer: Dry deposition and heterogeneous oxidation observed during the pacific atmospheric sulfur experiment," *J. Atmos. Chem.*, vol. 63, no. 1, pp. 13–32, May 2009, doi: 10.1007/s10874-010-9155-0.

[28] M. N. Deeter *et al.*, "The MOPITT Version 6 product: Algorithm enhancements and validation," *Atmos. Meas. Tech.*, vol. 7, no. 11, pp. 3623–3632, Nov. 2014, doi: 10.5194/amt-7-3623-2014.

[29] H. M. Worden *et al.*, "Decadal record of satellite carbon monoxide observations," *Atmos. Chem. Phys.*, vol. 13, no. 2, pp. 837–850, 2013, doi: 10.5194/acp-13-837-2013.

[30] A. Coppalle, V. Delmas, and M. Bobbia, "Variability of Nox and No2 concentrations observed at pedestrian level in the city centre of a medium sized urban area," *Atmos. Environ.*, vol. 35, no. 31, pp. 5361–5369, 2001, doi: https://doi.org/10.1016/S1352-2310(01)00296-5.

[31] B. N. Duncan *et al.*, "A space-based, high-resolution view of notable changes in urban NOx pollution around the world (2005–2014)," *J. Geophys. Res.*, vol. 121, no. 2, pp. 976–996, Jan. 2016, doi: 10.1002/2015JD024121.

[32] E. J. Good, D. J. Ghent, C. E. Bulgin, and J. J. Remedios, "A spatiotemporal analysis of the relationship between near-surface air temperature and satellite land surface temperatures using 17 years of data from the ATSR series," *Journal of Geophysical Research: Atmospheres*, vol. 122, no. 17, pp. 9185–9210, Sep. 2017, doi: 10.1002/2017JD026880.